broad but minor anomaly is also found in the dielectric permittivity at about 340 K over a range of frequencies. The transition, which appears to be second or higher order and rather gradual, is comparable to those often found in glasses.

$K_3Fe_5F_{15}$

The dielectric permittivity in $K_3Fe_5F_{15}$ passes through a sharp anomaly at 495 (10) K as the dielectric loss undergoes a change in slope (Ravez *et al.*, 1989). The heat capacity exhibits a λ-type anomaly at 490 (10) K, with an entropy change of 5·5 (2) J mol^{-1} K^{-1}; the value calculated from the predicted change in structure is 5·42 J mol^{-1} K^{-1}. The ferroelastic domains disappear abruptly on heating above 490 (10) K and reappear on cooling below 480 (10) K.

Nonferroelectric structures determined in *Pba2*

The atomic coordinates of $Au_2(SeO_3)_2O$, $K[Al_2F(H_2O)_4(PO_4)_2]$ and $Mn(NH_2NHCOO)_2(H_2O)_2$ are listed by ICSD in space group *Pba2*, in addition to those mentioned in the *Introduction* and those predicted above to be ferroelectric. These final three structures do not satisfy the criteria for ferroelectricity.

Additional entry in ICSD release of 1988

The structure of $In_2Ga_2Fe_2O_9$, reported by Nodari, Malaman & Evrard (1985), forms the 21st entry in space group *Pba2* of ICSD. With unit-cell dimensions, at room temperature, of $a = 19·253$ (3), $b = 7·2176$ (2) and $c = 3·2581$ (1) Å, 420 independent reflections with $I > 3\sigma(I)$ were measured by means of Ag $K\alpha$ radiation; absorption corrections were neglected as were anomalous-dispersion corrections. Refinement of a model with isotropic thermal parameters for all atoms gave $R = 0·037$. An origin translation along the c axis by 0·323 reveals that no atom is displaced from a mirror plane at $z = 0$ or $\frac{1}{2}$ by more than 2·8 e.s.d. It may hence be concluded that the given structure does not differ significantly from the alternative arrangement in space group *Pbam* in which atoms In(1), Fe(3), Ga(3), O(1) and O(5) have $z = 0$ and the remaining atoms have $z = \frac{1}{2}$. The structure, with maximum atomic displacement by a metal atom of 0·033 Å from a mirror plane, is hence not predicted to be ferroelectric; further structural investigation is appropriate.

References

ABRAHAMS, S. C. (1988). *Acta Cryst.* B**44**, 585–595.

ABRAHAMS, S. C., BRANDLE, C. D., BERKSTRESSER, G. W., O'BRYAN, H. M., BAIR, H. E., GALLAGHER, P. K. & DROTNING, W. D. (1989). *J. Appl. Phys.* **65**, 1797–1799.

ABRAHAMS, S. C., KURTZ, S. K. & JAMIESON, P. B. (1968). *Phys. Rev.* **172**, 551–553.

AURIVILLIUS, B. (1966). *Ark. Kemi*, **25**, 505–515.

CRAIG, D. C. & STEPHENSON, N. C. (1971). *J. Solid State Chem.* **3**, 89–100.

Crystallographic Databases (1987). Chester: International Union of Crystallography.

GENS, A. M., VARFOLOMEEV, M. B., KOSTOMAROV, V. S. & KOROVIN, S. S. (1981). *Zh. Neorg. Khim.* **26**, 896–898.

HARDY, A.-M., HARDY, A. & FEREY, G. (1973). *Acta Cryst.* B**29**, 1654–1658.

JAMIESON, P. B. & ABRAHAMS, S. C. (1968). *Acta Cryst.* B**24**, 984–986.

KEVE, E. T. & SKAPSKI, A. C. (1971). *J. Chem. Soc. A*, pp. 1280–1286.

KIHLBORG, L. (1960). *Acta Chem. Scand.* **14**, 1612–1622.

KIHLBORG, L. (1963). *Acta Chem. Scand.* **17**, 1485–1487.

MATVEEVA, R. G., VARFOLOMEEV, M. B. & IL'YUSHCHENKO, L. S. (1984). *Zh. Neorg. Khim.* **29**, 31–34.

NEVSKII, N. N., IL'YUKHIN, V. V., IVANOVA, L. I. & BELOV, N. V. (1979). *Dokl. Akad. Nauk SSSR*, **245**, 110–113.

NODARI, I., MALAMAN, B. & EVRARD, O. (1985). *Mater. Res. Bull.* **20**, 687–695.

RAVEZ, J., ABRAHAMS, S. C. & DE PAPE, R. (1989). *J. Appl. Phys.* In the press.

YAMAZOE, N., EKSTRÖM, T. & KIHLBORG, L. (1975). *Acta Chem. Scand Ser. A*, **29**, 404–408.

Acta Cryst. (1989). B**45**, 232–240

Electron Density Distribution in Cs_3CoCl_5

BY BRIAN N. FIGGIS,* EDWARD S. KUCHARSKI AND PHILIP A. REYNOLDS

School of Chemistry, University of Western Australia, Nedlands, Western Australia 6009, *Australia*

(*Received* 22 *January* 1988; *accepted* 18 *January* 1989)

Abstract

An X-ray diffraction data set was collected at 115 K from a crystal of Cs_3CoCl_5, which contains the $CoCl_4^{2-}$ anion. A 63-parameter multipole analysis based upon 1713 unique reflections of wavevector $< 1·08$ Å^{-1} yielded $wR(I) = 0·026$ with $\chi^2 = 0·731$; $R(F) = 0·013$ for 1384 data with $I > 3\sigma(I)$. The multipole parameters are consistent with the cobalt $3d$ orbital expanded radially by 7 (1)% and populated $e^{4·3(2)}t_2^{3·2(2)}$. The

* To whom correspondence should be addressed.

0108-7681/89/030232-09$03.00

model includes thin shells of density at about the van der Waals radii, and they make the definition of atomic charges on the Cs atoms and of covalence in the Co–Cl bonding unclear. The populations of these shells are substantial for Cs, 1·0 (1) e, but lower for Co, −0·2 (1) e, and Cl, 0·2 (1) e. The shells may be associated with the transfer of the outermost electrons of atoms into 'interstices' between the formal ions that make up the crystal. Crystal data: tricaesium cobalt pentachloride, $M_r = 635{\cdot}4$, tetragonal, $I4/mcm$, $a = 9{\cdot}123$ (4), $c = 14{\cdot}499$ (5) Å, $V = 1207$ (1) Å^3, $Z = 4$, $D_x = 3{\cdot}49$ Mg m^{-3}, λ(Mo $K\bar{\alpha}$) = 0·71069 Å, $\mu = 11{\cdot}55$ mm^{-1}, $T = 115$ (4) K.

1. Introduction

X-ray and polarized neutron diffraction (PND) experiments can provide detailed information about charge and spin densities, and so provide stringent tests of bonding theories in transition-metal complexes (Figgis & Reynolds, 1986). We have chosen to study the $CoCl_4^{2-}$ ion since it is small enough that one may perform good quality *ab-initio* calculations, and it forms simple well-behaved crystals, suitable for both X-ray and PND experiments. There is an excellent PND data set available for Cs_3CoCl_5 (Chandler, Figgis, Phillips, Reynolds & Williams, 1982). The spin density in its $CoCl_4^{2-}$ fragment has been compared with theoretical calculations on the free ion (Chandler *et al.*, 1982; Chandler & Phillips, 1986; Johansen & Andersen, 1986) with good qualitative but poor quantitative agreement.

The Cs_3CoCl_5 crystal has been studied, with increasing accuracy, by both X-ray (Powell & Wells, 1935; Figgis, Gerloch & Mason, 1964*a*; Reynolds, Figgis & White, 1981) and neutron diffraction (Figgis, Mason, Smith & Williams, 1980; Williams, Figgis & Moore, 1980) methods at room temperature and at 4·2 K. These studies reveal no phase change and so conform with heat capacity (Wielinga, Blote, Roest & Huiskamp, 1967), magnetic (Figgis, Gerloch & Mason, 1964*b*; Van Stapele, Beljers, Bongers & Zijlstra, 1966; Mess, Lagendijk, Curtis & Huiskamp, 1967), ESR (Van Stapele *et al.*, 1966; Beljers, Bongers, Van Stapele & Zijlstra, 1964) and optical spectroscopy (Bird, Cooke, Day & Orchard, 1974; Pelletier-Allard, 1964) measurements.

An extensive room-temperature X-ray study of Cs_3CoCl_5 showed sufficient anharmonicity in the thermal motion that only rudimentary charge density information could be deduced (Reynolds *et al.*, 1981). A recent low-temperature charge density study of the Cs_2CoCl_4 crystal (Figgis, Reynolds & White, 1987), which also contains the $CoCl_4^{2-}$ ion, gives qualitative agreement with theory. The charge deformation density seems to be as much affected by the 'non-bonded' Cs–Cs, Cs–Cl and Cs–Co interactions as the 'bonded' Co–Cl covalent ones.

In this paper we present a charge density quality X-ray data set on Cs_3CoCl_5, collected at 115 (4) K, and its analysis in terms of an augmented multipole model.

2. Experimental

Deep-blue rectangular prismatic crystals of Cs_3CoCl_5 were grown by rapidly cooling a warm aqueous solution of $CoCl_2.6H_2O$ containing CsCl in 5:1 molar ratio. A complete sphere of data to $2\theta = 100°$ was collected on a Syntex $P2_1$ diffractometer under the conditions of Table 1(*a*). Changes in the six standards employed appeared random and were less than 2%. Unit-cell parameters were determined from 14 reflections ($7{\cdot}2 \le \theta \le 11{\cdot}3°$).

During the data collection the crystal inadvertedly warmed to near ambient temperature and was reduced slightly in mass. A considerable section of the earlier data was subsequently collected again. The data thus consists of two sections of roughly equal extent, *A* and *B*, with much overlap.

3. Data processing

We have adopted an empirical approach in making our corrections for the experimental errors associated with absorption, extinction and multiple scattering. The absorption and extinction corrections are expected to affect Friedel equivalents equally. We obtained an agreement between Friedel equivalents of $R(I) = 0{\cdot}019$ (*A*) and 0·017 (*B*). Here $R(I) = \sum|I - \text{av.}(I)|/\sum\text{av.}(I)$, where av. indicates the arithmetic mean.

3.1. *Absorption*

To correct for absorption in this highly absorbing material we refined the crystal dimensions so as to optimize the agreement between suitable equivalent reflections using an analytical absorption correction. We used about 1800 moderate intensity reflections with $\theta < 20°$ and $3\sigma(I) < I < 80000$ counts, as described in Table 1(*b*). The refined and measured crystal dimensions were the same to within the accuracy of measurement.

3.2. *Multiple scattering*

We used an empirical correction for the effects of multiple scattering as suggested by the work of Le Page & Gabe (1979). We put

$$I(\text{obs.}) = I(\text{calc.}) + m_1 + m_2(1{\cdot}0 - |\mathbf{K}|) \qquad (1)$$

where **K** is the wavevector in Å^{-1}. This multiple-scattering correction affects all equivalents equally and is small, so it is introduced only in the refinement of the unique data.

3.3. *Anisotropic extinction*

We also developed an empirical procedure to correct for anisotropic extinction. We write the intensity reduction factor for extinction in a reflection, neglecting terms higher than unity in x, as (Becker & Coppens, 1974)

$$y = (1 + 2x)^{-1/2} \qquad (2)$$

where

$$x = C_e I(\text{calc.}) e t (\sin 2\theta)^{-n}. \qquad (3)$$

Here, I(calc.) is the 'ideal' calculated intensity, e is the extinction parameter, and t the path length for the reflection at the scattering angle θ. $n = 0$ or 1, depending on whether the extinction is dominated by the mosaic spread (type I) or the size (type II) of the crystal. C_e includes all those factors independent of the reflection indices, such as the X-ray wavelength and the cell volume.

Anisotropy in y arises through both the factors t and e. e may be a function of an experimental vector, **D** for type I, or **N** for type II extinction. **D** is a unit vector perpendicular to the scattering plane, **N** one in the scattering plane and perpendicular to the incoming beam. In conventional procedure each such vector modifies a tensor extinction parameter to give a different value of e for each reflection (Coppens & Hamilton, 1970; Thornley & Nelmes, 1974).

Empirically, we expand the parameter e in terms of the four diffractometer angles. In the present experiment only three of the diffractometer angles are independent, since $\omega = 2\theta$. Consequently, e is a function only of θ, χ and φ. **D** depends only on φ and χ but **N** depends on all three angles, varying only slowly with θ. Also, extinction affects higher-angle reflections only slightly. A χ and φ set specifies a particular direction in the crystal, so we write e as a function only of $\mathbf{K}/|\mathbf{K}|$ for each reflection. We expand e as a multipole function in the polar angles defined with respect to c and the ab plane as

$$e = \sum e_{lm} y_l^m \qquad (4)$$

where y_l^m are real spherical harmonic angular functions specified by l and m as conventionally used in multipole refinements. They are defined in terms of the complex spherical harmonics Y_l^m as follows:

$$y_l^m = \text{Re}(Y_l^m) \quad m \geq 0$$
$$y_l^m = i\text{Im}(Y_l^m) \quad m < 0. \qquad (5)$$

That expression is readily implemented in a conventional crystallographic least-squares program. It is a real tensorial expression, and need only be expanded to second-order terms for either type I or type II extinction. The resultant six parameters duplicate the angular dependence of type I conventional refinements and those of type II to a good approximation. It is very simple to use additional multipoles to allow for other domain angular distributions or nonellipsoidal crystal-domain shapes.

Table 1. *Crystal data and experimental parameters for* Cs_3CoCl_5

(*a*) Crystal data and diffractometer parameters

Space group	*I*4/*mcm*	
Temperature (K)	115 (4)	
Unit-cell lengths (Å)	$a = 9{\cdot}123$ (4)	$c = 14{\cdot}499$ (5)
At 295 K*	9·232 (2)	14·554 (2)
At 4·2 K†	9·063 (5)	14·450 (10)
U (Å^3)	1207 (1)	
Z	4	
D_x (Mg m^{-3})	3·49	
$(\sin\theta/\lambda)_{max}$ (Å^{-1})	1·08	
λ(Mo $K\bar{\alpha}$) (Å)	0·71069	
μ (mm^{-1})	11·55	
Scan mode	ω–2θ	
Scan angle (°)	1·9 + (α_1, α_2)	
Monochromator	Graphite plate (002)	
Background	0·5 of scan time	
Standards	Six every 100 reflections	

(*b*) Experimental parameters for data parts *A* and *B*

	Part *A*	Part *B*
Refined crystal dimensions (mm) (from centre)		
(001)–(00$\bar{1}$)	0·082	0·081
(110)–($\bar{1}\bar{1}$0)	0·079	0·078
(1$\bar{1}$0)–($\bar{1}$10)	0·095	0·095
(1$\bar{1}$2)–($\bar{1}$1$\bar{2}$)	0·104	0·102
Mean path length (mm)	0·085–0·159	0·085–0·159
hkl range	0–13, 0–30, 0–18	0–13, 0–30, 0–18
Transmission factors	0·17–0·29	0·18–0·29
No. of reflections measured	27386	20764
$R(I)$ (av. Friedel pairs)	0·019	0·017
$R(I)$ (av. equivalents)	0·021	0·025
$R(I)$ (merge *A* and *B*)	0·011	
No. of unique reflections	1724	

* Reynolds *et al.* (1981).
† Figgis *et al.* (1980).

Different mosaic-spread distributions alter the form of the extinction correction, introducing higher powers of x (Becker & Coppens, 1974). We find a term proportional to I^2 is statistically significant, but small. We include it as a refinable isotropic parameter, f. Thus we have a final extinction correction

$$y = (1 + 2x + fx^2)^{-1/2}. \qquad (6)$$

We refined our anisotropic extinction model using the Friedel-pair-averaged data (not a final unique set), varying only the extinction multipole terms e_{lm} with lm = 00, 20, 21, 21̄, 22, 22̄, 40, 44, and employing the 190 (*A*) and 264 (*B*) most intense reflections. The values of l and m important in the final averaged unique intensities were selected using the following arguments. For l odd, x in (2) is of the same magnitude for Friedel pairs, since t is the same, but is of opposite sign. Thus, provided $x \ll 1{\cdot}0$, the averaging of Friedel pairs almost cancels the effects of the l-odd poles. Similarly, the values of the l-even parameters, e_{lm}, lm = 21, 21̄, 22, 22̄, are sensitive to the differences between non-Friedel-pair equivalents, but after averaging in the 4/*mmm* Laue symmetry, the mean 'unique' intensity is affected to a small extent by these parameters because x changes sign between equivalents and in addition t may differ between them. In contrast, the multipoles lm = 00 and 20 affect the

unique reflection intensities strongly since all equivalents have the same sign of x. Of the fourth-order multipoles, only $lm = 40$ and 44 have the same sign of x over all equivalents. We also include these but neglect the other seven fourth-order multipoles since, as for $lm = 21$, $2\bar{1}$, 22 and $2\bar{2}$, for a relatively isotropic crystal with x small, the corrections will partly cancel on averaging the equivalents. We also assume that the sizes of the fourth-order terms are smaller than those of second order, and that the sixth- and higher-order multipole terms are negligible. Thus, given some variation in t between equivalents, we may estimate that the eight parameters chosen are those that affect the final averaged unique reflection intensities most strongly.

We obtained agreement factors of $R(I) = 0{\cdot}026$ (A), $0{\cdot}022$ (B); $R(F) = 0{\cdot}012$ (A), $0{\cdot}015$ (B). The average values obtained for the extinction parameters, were (set A given first): e_{00} 640 (15), 326 (10); e_{20} 51 (7), 65 (8); e_{21} 127 (21), 77 (25); $e_{2\bar{1}}$ 8 (21), 86 (30); e_{22} 34 (10), 47 (11); $e_{2\bar{2}}$ 291 (21), 130 (15); e_{40} 84 (10), 13 (5); e_{44} −52 (11), −54 (10). Type I extinction gave marginally better agreement factors than type II, and was used. Eleven reflections, with $y < 0{\cdot}65$ (minimum 0·35) in set A, had sufficiently large extinction corrections that they were likely to bias refinements and so were omitted from subsequent refinement.

3.4. *Averaging the data*

We averaged the equivalent extinction-corrected reflections in each data set, and the agreement factors are given in Table 1. Using common reflections the two sets were then combined by refinement of a scale factor with weighted averaging, giving merging $R(I) = 0{\cdot}011$. There resulted 1724 final unique reflections, a complete set to $|\mathbf{K}| = 1{\cdot}08$ Å^{-1}.

4. Refinements of unique data

We refined the thermal and positional parameters, some experimental parameters, and a flexible-multipole valence-electron-density model simultaneously, noting that unacceptable correlation between parameters did not arise. We included in the refinements those parameters concerned with absorption, extinction and multiple scattering which were not well defined by the agreement of equivalents. For absorption we introduced a term containing the spherical harmonic y_2^0 into the scale factor, which became

$$s = s_{00} + s_{20}y_2^0. \quad (7)$$

For extinction, in addition to the quadratic isotropic term, we refined those multipolar terms not partially cancelled by averaging over equivalent reflections, giving a correction of the form

$$e = e_{00} + e_{20}y_2^0 + e_{40}y_4^0 + e_{44}y_4^4 + fx^2. \quad (8)$$

Table 2. *Results of refinement of the data for* Cs_3CoCl_5 *with various models*

	Multipole		Spherical atom
	R1	R1′	R2
sin θ/λ range (Å^{-1})	0–1·08	0–0·7	0–0·7
No. of reflections	1713	485	485
No. of observed reflections $[I > 3\sigma(I)]$	1384	454	454
No. of parameters	63	—	9
$R(I)$	0·0179	0·0134	0·0216
$wR(I)$	0·0261	0·0172	0·0233
$R(F)$ $[I > 3\sigma(I)]$	0·0129	0·0074	0·0100
χ^2	0·731	0·748	1·010

Since small shifts might be expected with use of a valence-electron model, the original extinction parameters e_{00}, e_{20}, e_{40}, e_{44} and f, derived using a conventional spherical-atom model, were included in the new refinements. The other extinction parameters affect equivalent reflections unequally and so are much less sensitive to the electron model used: they were not further refined.

A posteori, as a check on the procedure, we performed a conventional spherical-atom refinement of data with $|\mathbf{K}| > 0{\cdot}7$ Å^{-1} using form factors listed in a standard compilation (Ibers & Hamilton, 1974). No difference in thermal or positional parameters was more than four standard deviations.

4.1. *Deformation density – multipole model*

On each Cs atom we placed a 54-electron Cs^+ core and a multipole set of $5p$ radial dependence obtained from theoretical calculations, as described previously (Figgis *et al.*, 1987). All four Cs(1) and nine Cs(2) multipoles allowed in the respective site symmetries 422 and $mm2$ up to order four were allowed to vary. On the Co-atom site ($\bar{4}2m$) four $3d$ orbital populations and five diffuse multipole populations up to order four were allowed to refine. The $3d$ and the diffuse form factors were derived from a $3d^7 4p^1$ Co^+ atomic calculation. The diffuse multipoles were given $4p$ radial dependence. The $3d$ populations introduced were the e and t_2 sets, with additional $3d_{xy}$ and $3d_{z^2}$ components to express any deviations from cubic symmetry. On Cl(1) ($4/m$ site) both, and on Cl(2) (m site) all six, allowed multipoles up to order two, with $3p$ radial dependence, were allowed to vary. On the Co and Cl atoms the $3d$ or $3p$ radii, respectively, were refined but the diffuse $4p$-like multipoles on the Co atom had a fixed radial dependence. In addition, on each atom, i, the population of an infinitely thin spherical shell was included (p^i_{shell}). The form factor, associated with a spherical density concentrated at r from the atom centre, is given by Kasper & Lonsdale (1967):

$$f(s) = \sin(2\pi r|\mathbf{K}|)/(2\pi r|\mathbf{K}|) \quad (9)$$

where r is the shell radius which was taken as 1·5 Å for all atoms for the refinements reported in this paper.

The parameters of the model were refined by full-matrix least-squares procedures on all 1713 unique

Table 3. *Positional* ($\times 10^5$) *and equivalent isotropic thermal parameters* ($Å^2 \times 10^4$) *for* Cs_3CoCl_5 *from refinement R*1, *compared with the* 295 K (*second entry*) *and* 4·2 K (*third entry*) *results*

Symmetry-determined values are given with no e.s.d. (first entry) or are omitted.

$$U_{eq} = \tfrac{1}{3} \sum_{i=1}^{3} U_{ii}.$$

	x	y	z	U_{eq}
Co(1)	0	50000	25000	87
				294
				27
Cs(1)	0	0	5000	142
				144
				34
Cs(2)	66324 (1)	16324	0	102
	66575 (5)			329
	66225 (7)			24
Cl(1)	0	0	0	126
				393
				50
Cl(2)	14150 (4)	64150	15722 (2)	153
	13915 (10)		15760 (11)	472
	14210 (3)		15711 (2)	52

Table 4. *Experimental parameters determined from refinement R*1

Scale	s_{00}	3·559 (4)	s_{20}	0·011 (3)
Multiple scattering	m_1	248 (13)	m_2	1093 (80)
Extinction	e_{00}	168 (18)	e_{20}	−2 (6)
	e_{40}	38 (8)	e_{44}	−5 (9)
	f	−0·38 (6)		

data, using the standard deviations obtained from the averaging of equivalent reflections for the weighting scheme, and constraining the value of the [000] 'reflection' to be 1104·61. The function minimized was $w[I(\text{obs.}) - I(\text{calc.})]^2$, where $w = \sigma[I(\text{obs.})]^{-2}$. We call this refinement R1 and it is described in Table 2. χ^2 was 0·731. Its positional and thermal parameters are given in Table 3,* the extinction and other experimental parameters in Table 4, and the valence and multipole parameters in Table 5. We emphasize that these extinction parameters are *shifts* from the values applied previously to the Friedel-pair-averaged data. For reference with work to follow, we repeated this refinement using data with $|\mathbf{K}| < 0{\cdot}7$ Å^{-1}, and the results, with $\chi^2 = 0{\cdot}748$, are listed as R1′ in Table 2.

The negligible value for the anisotropic 'scale-factor' parameter s_{20} implies that the initial correction for absorption was satisfactory. The multiple-scattering corrections are small, positive and decrease with $|\mathbf{K}|$ as required. The only significant change in the earlier highly anisotropic extinction parameters introduced by R1 is a small one in the isotropic component e_{00}. The

Table 5. *Valence parameters determined from refinement R*1

Cs(1)	(00)	(20)	(40)	(44)
	−0·4 (2)	−0·9 (3)	0·0 (2)	0·6 (3)
	p_{shell}			
	1·0 (1)			
Cs(2)	(00)	(10)	(20)	(22)
	−0·5 (1)	−0·1 (2)	0·3 (2)	−0·5 (3)
	(30)	(32)	(40)	(42)
	−0·2 (1)	0·5 (2)	−0·4 (2)	−0·8 (2)
	(44)	p_{shell}		
	0·1 (2)	0·9 (1)		
Co(1)	$3d$–e	$3d$–t_2	$3d_{xy}$	$3d_{z^2}$
	4·3 (2)	3·2 (2)	0·1 (1)	−0·2 (1)
	(00)	(20)	(3–2)	(40)
	0·9 (3)	0·0 (2)	0·1 (3)	0·1 (2)
	(44)	p_{shell}	r_{3d}	
	0·2 (3)	−0·2 (1)	1·07 (2)	
Cl(1)	(00)	(20)	p_{shell}	r_{3p}
	7·4 (2)	−0·3 (1)	0·1 (1)	0·95 (1)
Cl(2)	(00)	(10)	(11)	(20)
	7·1 (1)	0·1 (1)	0·2 (1)	0·0 (1)
	(21)	(22)	p_{shell}	r_{3p}
	0·0 (1)	0·0 (1)	0·3 (1)	0·98 (1)

new isotropic quadratic component parameter, f, is −0·38 (6). Compare this with values for Gaussian (1·30), Lorentzian (0·31) and Fresnel (1·08) models of mosaic distribution in the crystal (Becker & Coppens, 1974). As is most usually the case the Lorentzian distribution provides the best fit (Coppens, 1978).

As a benchmark with which to compare R1 and subsequent refinements, which will be presented in a separate paper, we performed another using spherical-atom form factors for Cs^+, Co^{2+} and Cl^- taken from a standard compilation (Ibers & Hamilton, 1974) and the data with $|\mathbf{K}| < 0{\cdot}7$ Å^{-1}. Positional, thermal and the nine experimental parameters of Table 4 were refined to give the results listed as R2 in Table 1, with $\chi^2 = 1{\cdot}010$. Note that the charge modelling in R1 produces a very significant improvement in fit to R2.

Fig. 1. Deformation charge density map for the $z = 0$ plane of Cs_3CoCl_5, containing Cl(1) and Cs(2). The contour interval in this and subsequent maps is 0·2 e Å^{-3}; solid lines for positive, dashed lines for negative density. The plane extends from $x = 0$ to 0·5 and from $y = 0$ to 0·5, downwards, the complete unique area in the plane.

* Lists of anisotropic thermal parameters, structure factors and charge deformation around atoms for various radii of integration have been deposited with the British Library Document Supply Centre as Supplementary Publication No. SUP 51605 (13 pp.). Copies may be obtained through The Executive Secretary, International Union of Crystallography, 5 Abbey Square, Chester CH1 2HU, England.

The room-temperature X-ray structural study of Cs_3CoCl_5 indicated significant anharmonicity in the thermal motion (Reynolds *et al.*, 1981). An extension of refinement R1 to include anharmonic parameters yielded a negligible improvement in χ^2 and no significant anharmonicity, presumably because of the lower experimental temperature.

Figs. 1–3 show deformation density maps based upon refinement R2 and calculated in three planes. The first plane has $z = 0$ and contains Cl(1) and Cs(2), the second has $z = 0{\cdot}25$ and contains Co(1) and Cs(1), the third is (110) and contains Co(1) and Cl(2).

4.2. *Direct form-factor analysis of the data*

The least-squares fitting of models to the data has the limitation that unexpected features of the deformation density may not be modelled. The multipole components of the form factors of charge density within spheres of radius r centred at r_0 may be computed directly from the data by means of the summation (Vidal-Vilat, Vidal & Kurki-Suonio, 1978):

$$f_{lm}(|\mathbf{K}|,r,\mathbf{r}_0)=\sum_j y_l^m(16\pi^2r^3/V)q_l(2\pi r|\mathbf{K}|,2\pi r|\mathbf{K}_j|) \times \exp(-2\pi i\mathbf{K}_j.\mathbf{r}_0).F_j \quad (10a)$$

where

$$q_l(x,y) = [xj_{l+1}(x)j_l(y) - yj_{l+1}(y)j_l(x)]/(x^2-y^2). \quad (10b)$$

$\mathbf{K}_j$ is the wavevector for the jth reflection, V is the cell volume, $j_l(x)$ is the lth-order Bessel function and y_l^m is the normalized spherical harmonic, in the usual nomenclature. F_j is the structure factor, with sign, for the cell, which is assumed to be centrosymmetric. To minimize truncation errors arising from neglect of high $|\mathbf{K}_j|$ reflections we employ the deformation difference function $(F_j - F_j^s)$ in our calculations modifying (10) and (11) accordingly. F_j^s is the structure for reflection j calculated on the spherical-atom model, corresponding to refinement R2. The sign of F_j is taken to be the same as that of F_j^s.

A series related to that above gives the total charge inside a sphere of radius r centred at r_0:

$$Z(r,\mathbf{r}_0) = \sum_j(4\pi r^3/V)F_j j_1(2\pi|\mathbf{K}_j|r)(2\pi|\mathbf{K}_j|r)^{-1} \times \exp(-2\pi i\mathbf{K}_j.\mathbf{r}_0). \quad (11)$$

Associated with these series are the random errors corresponding to the standard deviations of the structure factors and the systematic errors, of which the most important involves the scale factor.

The use of all reflections in the summations means that these series are sensitive to errors in particular parts of the data – in our case the eleven reflections highly affected by extinction. In the least-squares procedure such poorly determined data can often be omitted with little penalty. Thus, although these direct treatments of the data are less biased they are not capable of as accurate an analysis of a given data set as a well constructed model.

We use (11) to investigate charge shifts from the ionic model of Cs^+, Co^{2+}, Cl^- (radial dependence as used in the multipole refinement) at the five atomic sites, using all the data. In the deposited material the relevant values are listed as a function of radius around each atom site. There is substantial noise in these lists, but a clear trend is present. All atoms except Co lose about 1 e from a radius varying from 1·4 to 2·4 Å from the nucleus, with little change nearer to that. The Co atom appears to lose about 0·5 e from the region 0·4 to 0·8 Å from the nucleus. The loss of charge at atomic sites must be compensated by an increase elsewhere. Similar expansions about interstitial sites such as (0·125,0·125,0) showed positive charge accumulation there. However, there are many such interstices and the amount of charge at each was too small to quantify well.

Fig. 2. Deformation charge density map for the $z = 0{\cdot}25$ plane of Cs_3CoCl_5, containing Co(1) and Cs(1), with x and y defined as in Fig. 1.

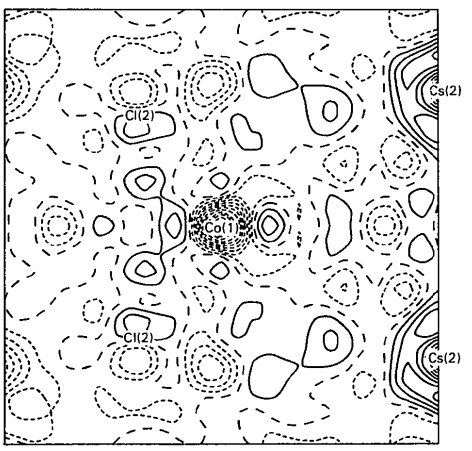

Fig. 3. Deformation charge density map for the (110) plane of Cs_3CoCl_5, containing Co(1), Cs(2) and Cl(2).

In order to further substantiate the redistribution of diffuse charge we employed (10) with spheres of radii 1·25, 1·75 and 2·25 Å summing to $|\mathbf{K}| = 0{\cdot}7$ Å^{-1}. The spherical components of the resulting form factors, y_0^0, are plotted in Fig. 4. Some aspherical terms were calculated also, ($y_2^0 y_4^0 y_4^{\pm 4}$), but were found to be much smaller. The errors associated with the curves of Fig. 4 are about 0·2 e.

5. Results and discussion

5.1. *Crystal structure and interionic forces*

In the earlier study on Cs_2CoCl_4 we suggested that the deformation density for an atom is closely correlated with the nearest neighbour ions, whether 'bonded' or 'non-bonded', and that the associated features can be quite localized. The significantly short interionic distances in Cs_3CoCl_5 are listed in Table 6 for each atom in ascending order of δD, the deviation from the sum of the ionic radii of the constituent ions. The ionic radii used (Cs^+ 1·7, Cl^- 1·8, Co^{2+} 0·75 Å) are consistent with those of Shannon (1976). The remaining contacts are significantly longer, with $\delta D = ca$ 0·6 Å for some Cl—Cl vectors.

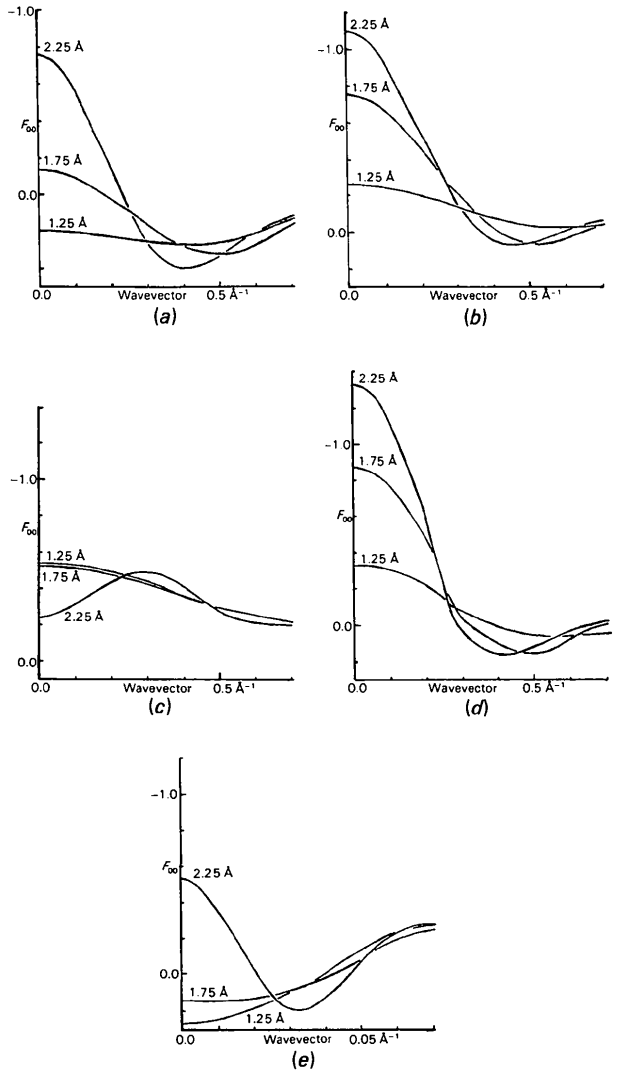

Fig. 4. Spherical component of the form factor *versus* wavevector for atomic sites: (*a*) Cs(1), (*b*) Cs(2), (*c*) Co, (*d*) Cl(1), (*e*) Cl(2). The radius of the sphere of integration of charge is indicated near each curve.

Table 6. *Short interionic vectors in* Cs_3CoCl_5

δD is defined as the observed distance minus the sum of the ionic radii.

	Vector	δD (Å)	Coordination No.
Co(1)	Co(1)–Cl(2)	−0·28 (1)	4
Cs(1)	Cs(1)–Cl(1)	0·12 (1)	2
	Cs(1)–Cl(2)	0·26 (1)	8
Cs(2)	Cs(2)–Cl(2)	−0·10 (1)	2
	Cs(2)–Cl(1)	−0·09 (1)	2
	Cs(2)–Cl(2)	0·10 (1)	4
Cl(1)	Cl(1)–Cs(2)	−0·09 (1)	4
	Cl(1)–Cs(1)	0·12 (1)	2
Cl(2)	Cl(2)–Co(1)	−0·28 (1)	1
	Cl(2)–Cs(2)	−0·10 (1)	1
	Cl(2)–Cl(2)	0·05 (1)	1
	Cl(2)–Cs(2)	0·10 (1)	2
	Cl(2)–Cl(2)	0·12 (1)	2
	Cl(2)–Cs(1)	0·26 (1)	2
	Cl(2)–Cl(2)	0·28 (1)	1

From Table 6 we see, that the short Co(1)–Cl(2) distance indicates significant interaction within the $CoCl_4$ fragment. At the other extreme, the Cs(1) ion appears to be in a cavity too large for its size. Examination of the short distances in Table 6 leads us to expect some 'intermolecular' effects on the valence electron distribution for Cl(1) and Cs(2) if the influences are of very short range.

For the X-ray data at 295 K, and now at 115 K, the average diagonal thermal parameters (U_{eq}) for atoms are in the order Co(1) < Cs(2) < Cl(1) < Cs(1) < Cl(2), indicating that the forces on each ion lie in the reverse order of magnitudes. Again, Cs(1) appears to be only weakly influenced by its neighbours. If we assume the effective mass is closer to the mass of the ion concerned than to the mean mass, then we obtain from the 4 K neutron data zero-point motion a force constant order Co(1) < Cs(2) < Cl(1) < Cl(2) < Cs(1). That is the same order as obtained from the higher-temperature data, apart from the inversion of Cl(2) and Cs(1), and indicates that deformation effects are weak for Cs(1) and Cl(2).

The mean ratios of the diagonal thermal-motion parameters at 295 and at 115 K lie between 3·09 and 3·38 for all five ions. The expected ratio is almost $295/115 = 2{\cdot}57$, so that, as assumed previously (Reynolds *et al.*, 1981), some anharmonicity in the motion appears to be present at least at room temperature.

From this analysis of structural parameters we conclude that the $CoCl_4$ fragment may expect significant deformation forces but otherwise 'intermolecular' effects in Cs_3CoCl_5 are weak. Cl(1) and

Cs(2) may be polarized to some extent but the electrostatic forces on Cs(1) are significantly weaker.

5.2. *Deformation density in an ionic crystal*

5.2.1. *Density maps.* The strongest features in the deformation density maps of Figs. 1–3 are around the ions and consist of slight excesses of density for Cs atoms and a deficit for Co and Cl(1), and are of approximately cylindrical symmetry. In particular, we see no 'bonding' density along the Co—Cl(2) vector and no evidence of the asphericity around the Co atom which should arise from an ideal $3d\ t_2^3e^4$ configuration.

In other systems, applications of anisotropic extinction have been found to flatten aspherical features around atoms. Such a correlation is absent here for the cobalt site for two reasons. Firstly, extinction operates on intensity, not on the cobalt *partial* structure factor. In this case the cobalt scattering is small compared with that of the Cs atoms. Secondly extinction is most important for low-angle reflections, whereas cobalt asphericity has its maximum effect around 0·7 Å^{-1}, near where the non-spherical component of the form factor, j_4 (Ibers & Hamilton, 1974), is maximum. Conversely where a single scattering centre dominates the scattering, anisotropic extinction *can* flatten diffuse anisotropic features. We conclude that the lack of aspherical features around the Co atom is not caused by poor correction for extinction but is a real feature of the charge density. For the Cs sites we cannot be so certain; extinction may have an effect on the asphericity, and in particular, diffuse features may be artificially reduced. In this case we may be affecting 6*p*-like features on the caesium. The short Cs(2)—Cl(1) vector in Fig. 1 and the short vector, almost along the Cs(2)—Cl(2) direction, in Fig. 3, contain no peaks along their lengths. The model residual maps from R1 (not shown) are almost featureless, as is to be expected from the results of a refinement with $R(F) = \sim 0{\cdot}01$. Only part of the hole at the Cl(1) positions remains.

In Cs_2CoCl_4 the deformation and residual density maps showed small peaks associated with short interionic vectors, such as Cs—Cl. We do not see any evidence of such features in the present maps for Cs_3CoCl_5.

5.2.2. *Ionic deformation and the direct summation.* The implementation of (10) indicates that the electron density of all atoms is depleted in a shell 1·4 to 2·4 Å from the nucleus and increased in regions of the cell remote from the atoms. Ten to thirty electrons may be involved for the cell, depending on the model used. The form-factor curves of Fig. 4 show this in a different way. The Co-atom curves are relatively flat and independent of the radius of integration, and correspond to little deformation of the free ion. The Cs- and Cl-atom curves show little change from the free ion below a 1·25 Å radius but then there is a rapid depletion of charge which continues through to the 1·75 Å mark. In all these curves there is a rapid increase from the initial negative values to a maximum significantly greater than zero at $|\mathbf{K}| \simeq 0{\cdot}4$ Å^{-1}. The curves can be seen to be consistent with the model which we employed earlier, in which a thin shell of density, varying in population from 0·3 to 1·3 e, was removed from a radius of ~ 1·3 Å around each atom to more diffuse regions.

The interpretation of these results in terms of conventional chemical-bonding pictures is uncertain. The amount of charge at radius r for Cs^+ 5*p* orbitals defined by 'good quality' wave functions (Clementi & Roetti, 1974) maximizes at 1·0 Å and drops to 35% at 1·75 Å. 50% of the charge corresponding to those orbitals lies within 1·2 Å of the nucleus and 86% within 1·75 Å. For Cl^- the non-bonded radius is 1·8 Å, the maximum charge density is at 0·8 Å, 50% of charge is within 1·0 Å and 89% within 1·75 Å. The diffraction results indicate that only the *outermost* part of such atomic valence densities are removed to interstices in the cell. For a close-packed lattice of ions of van der Waals radius 1·8 Å the maximum distance from a nucleus to the centre of a tetrahedral 'hole' is $1{\cdot}5^{0{\cdot}5} \times 1{\cdot}8 = 2{\cdot}2$ Å. Using the above Cs^+ 5*p* wave function, a density of 0·050 e Å^{-3} at such a site can be calculated. From these considerations and the direct-space analysis we can conclude that charge is removed from the 0·8 to 1·8 Å radial region of the Cs and Cl atoms, and reappears in the 1·8 to 2·2 Å region, with unknown distribution. In the following paper we attempt to model the unknown diffuse distribution by a least-squares analysis of some possible models.

6. Conclusions

The X-ray data at 115 K for Cs_3CoCl_5 may be corrected for absorption and extinction by empirical procedures to give a unique set of high accuracy. Anharmonicity may not be significant. Modelling of the data with a conventional multipole set is not entirely satisfactory. The fit is significantly improved if a shell of electron density at about the van der Waals radius is removed and the resulting charge distributed elsewhere, presumably in the 'interstices' between formal ions. This shell model makes any definition of ionic charge unreasonable.

Procedures for analytical integration of charge about atom centres support the reality of the shells and the delocalization of charge into very diffuse regions of the cell, but because of their dependence on completeness of the data, it is not possible to use them in a very quantitative fashion.

The authors are grateful to the Australian Research Grants Scheme for financial support and to the University Crystallography Centre for access to the $P2_1$ diffractometer.

References

BECKER, P. & COPPENS, P. (1974). *Acta Cryst.* A**30**, 129–147.
BELJERS, H. G., BONGERS, P. F., VAN STAPELE, R. P. & ZIJLSTRA, H. (1964). *Phys. Lett.* **12**, 81–82.
BIRD, B. D., COOKE, E. A., DAY, P. & ORCHARD, A. F. (1974). *Philos. Trans. R. Soc. London Ser. A*, **276**, 277–339.
CHANDLER, G. S., FIGGIS, B. N., PHILLIPS, R. A., REYNOLDS, P. A. & WILLIAMS, G. A. (1982). *Proc. R. Soc. London Ser. A*, **384**, 31–48.
CHANDLER, G. S. & PHILLIPS, R. A. (1986). *J. Chem. Soc. Faraday Trans.* 2, **82**, 573–592.
CLEMENTI, E. & ROETTI, C. (1974). *At. Data Nucl. Data Tables*, **14**, 177–478.
COPPENS, P. & HAMILTON, W. C. (1970). *Acta Cryst.* A**26**, 71–83.
COPPENS, P. (1978). In *Neutron Diffraction*, edited by H. DACHS. Berlin: Springer-Verlag.
FIGGIS, B. N., GERLOCH, M. & MASON, R. (1964*a*). *Acta Cryst.* **17**, 506–508.
FIGGIS, B. N., GERLOCH, M. & MASON, R. (1964*b*). *Proc. R. Soc. London Ser. A*, **279**, 210–228.
FIGGIS, B. N., MASON, R., SMITH, A. R. P. & WILLIAMS, G. A. (1980). *Acta Cryst.* A**36**, 509–512.
FIGGIS, B. N. & REYNOLDS, P. A. (1986). *Int. Rev. Phys. Chem.* **5**, 265–272.
FIGGIS, B. N., REYNOLDS, P. A. & WHITE, A. H. (1987). *J. Chem. Soc. Dalton Trans.* pp. 1737–1745.
IBERS, J. & HAMILTON, W. C. (1974). Editors. *International Tables for X ray Crystallography*, Vol. 4. Birmingham: Kynoch Press. (Present distributor Kluwer Academic Publishers, Dordrecht.)
JOHANSEN, H. & ANDERSEN, N. K. (1986). *Mol. Phys.* **58**, 965–975.
KASPER, J. S. & LONSDALE, K. (1967). In *International Tables for X-ray Crystallography*, Vol. 2. Birmingham: Kynoch Press. (Present distributor Kluwer Academic Publishers, Dordrecht.)
LE PAGE, Y. & GABE, L. J. (1979). *Acta Cryst.* A**35**, 73–78.
MESS, K. W., LAGENDIJK, E., CURTIS, D. A. & HUISKAMP, W. (1967). *Physica*, **34**, 126–148.
PELLETIER-ALLARD, N. (1964). *C. R. Acad. Sci.* **258**, 1215–1220.
POWELL, H. M. & WELLS, A. F. (1935). *J. Chem. Soc.* pp. 359–362.
REYNOLDS, P. A., FIGGIS, B. N. & WHITE, A. H. (1981). *Acta Cryst.* B**37**, 508–513.
SHANNON, R. D. (1976). *Acta Cryst.* A**32**, 751–767.
THORNLEY, F. R. & NELMES, R. J. (1974). *Acta Cryst.* A**30**, 748–757.
VAN STAPELE, R. P., BELJERS, H. G., BONGERS, P. F. & ZIJLSTRA, H. (1966). *J. Chem. Phys.* **44**, 3719–3725.
VIDAL-VILAT, G., VIDAL, J. P. & KURKI-SUONIO, K. (1978). *Acta Cryst.* A**34**, 594–602.
WIELINGA, R. F., BLOTE, H. W. J., ROEST, J. A. & HUISKAMP, W. J. (1967). *Physica*, **34**, 223–240.
WILLIAMS, G. A., FIGGIS, B. N. & MOORE, F. H. (1980). *Acta Cryst.* B**36**, 2893–2897.

Acta Cryst. (1989). B**45**, 240–247

Relation of the Electron Density Distribution in the $CoCl_4^{2-}$ Ion to the Spin Density and to Theory

BY BRIAN N. FIGGIS,* EDWARD S. KUCHARSKI AND PHILIP A. REYNOLDS

School of Chemistry, University of Western Australia, Nedlands, Western Australia 6009, *Australia*

(*Received* 7 *May* 1988; *accepted* 18 *January* 1989)

Abstract

Based upon the 115 K X-ray data for Cs_3CoCl_5 several valence-orbital refinements were carried out to elucidate features of chemical interest. They gave a $t_2^{3.9(2)}e^{4.2(2)}4s'^{0.4(3)}$ valence-electron configuration for the Co atom, when averaged to cubic symmetry. There is a substantial and important redistribution of charge within all ions, which can be well represented by a thin spherical shell at a radius of *ca* 1·50 Å from each nucleus, but not by any of a number of other models of diffuse density. Deviation from cubic symmetry for the Co atom is marked. The results are quite similar to those of an earlier study on Cs_2CoCl_4, and show the importance of effects in the Cs···Cl bonds reminiscent of covalency. The relationship between those charge density results and the spin density distribution obtained on the same compound by polarized neutron diffraction shows that an advanced level of theoretical treatment is required to account for both experiments.

1. Introduction

This paper draws on the results of the preceding paper (Figgis, Kucharski & Reynolds, 1989*a*) for the charge distribution in Cs_3CoCl_5, on the equivalent results for Cs_2CoCl_4 (Figgis, Reynolds & White, 1987), and on the experimental spin density distribution for Cs_3CoCl_5 (Chandler, Figgis, Phillips, Reynolds & Williams, 1982) to examine the bonding in the $CoCl_4^{2-}$ ion.

Complementary X-ray and polarized neutron diffraction (PND) studies have been made on $Cs_2K[Cr(CN_6)]$ (Figgis, Forsyth & Reynolds, 1987; Figgis & Reynolds, 1987), $(NH_3)_4Ni(NO_2)_2$ (Figgis, Reynolds & Wright, 1983; Figgis, Reynolds & Mason, 1983) and Co(pc) (Williams, Figgis & Mason, 1981; Figgis, Kucharski & Reynolds, 1989*b*) (pc=phthalocyaninato ion). Those systems, while having more chemical

* To whom correspondence should be addressed.

0108-7681/89/030240-08$03.00